Journal of Applied Polymer Science

Increased thermal stability of nanocellulose composites by functionalization of the sulfate groups on cellulose nanocrystals with azetidinium ions

Mikaela Börjesson [1], Karin Sahlin [1,2], Diana Bernin,[3] Gunnar Westman[1,2]
[1]Department of Chemistry and Chemical Engineering, Chalmers University of Technology, Gothenburg SE-41296, Sweden
[2]Wallenberg Wood Science Center (WWSC), Chalmers University of Technology, Gothenburg SE-41296, Sweden
[3]Swedish NMR Centre, University of Gothenburg, Gothenburg SE-40530, Sweden
Correspondence to: G. Westman (E-mail: westman@chalmers.se)

ABSTRACT: Cellulose nanocrystals (CNCs) prepared via sulfuric acid hydrolysis are decorated with sulfate groups that yield a stable water suspension. To make the CNCs adaptable for use in composites, the hydroxyl groups on the surface are usually hydrophobized. In this article, an alternative hydrophobization method is described in which the sulfate groups are conjugated with azetidinium salts. The results of this study show that the sulfate groups can be functionalized with azetidinium salts and from thermal studies, it was discovered that the functionalization led to a 100 °C increase in thermal stability, compared with unmodified CNCs. The nanocomposites prepared by extrusion of CNC-coated low-density polyethylene powder displayed similar mechanical properties as the CNC-reference sample, but without the discoloration, due to the increased thermal stability. In conclusion, the azetidinium reagent reacts preferentially with sulfate groups, and this new type of chemical conversion of sulfate groups on polysaccharides will be beneficial in nanocomposite manufacturing. © 2017 Wiley Periodicals, Inc. J. Appl. Polym. Sci. **2018**, *135*, 45963.

KEYWORDS: biopolymers and renewable polymers; cellulose and other wood products; functionalization of polymers; nanoparticles; nanowires and nanocrystals

Received 25 July 2017; accepted 20 October 2017
DOI: 10.1002/app.45963

INTRODUCTION

Cellulose sulfates are a relatively new cellulose derivative that have found application in biotechnical and medical applications.[1–3] They can be produced in different ways, such as by reacting cellulose with chlorosulfuric acid or sulfamic acid.[4,5] Sulfated cellulose nanocrystals (CNCs) are produced when cellulose is hydrolyzed with sulfuric acid, resulting in charged nanocrystals for which some of the surface hydroxyl (—OH) groups have been substituted with $-OSO_3^-$ groups, forming a stable aqueous CNC suspension.[6–9] The amount of charged sulfate groups on the crystal surfaces can be controlled or changed in different ways, either during the sulfuric acid hydrolysis or afterwards. There have also been reports in which hemicellulose from the process water at mills—that is, galactoglucomannans extracted from thermomechanical pulp—has been converted to sulfated derivates.[10–12]

Chemical modification of sulfated polysaccharides by means of desulfation, oversulfation, and acylation has been done in the literature in order to affect the properties of the polysaccharides. It is also well known that there is a relationship between sulfate content and the properties of a material.[13] Chemical modification via linkers that contain charges has shown that it is possible to obtain materials with thixotropic behavior.[14] Sulfated nanocellulose is very hydrophilic; consequently, it is difficult to disperse this material in the more hydrophobic precursors of thermosets and thermoplastics in order to produce biocomposites. To enhance the chemical compatibility between CNCs and a matrix, the CNCs are usually hydrophobized. This can be done either by the adsorption of a hydrophobic cation by the sulfate groups, or by chemical modification of the CNC surfaces.[15–17] Chemical modification of the CNC surface is usually performed via functionalization of the hydroxyl groups on the surface. This functionalization results in a more hydrophobic material, but still leaves the CNC with negatively charged sulfate groups with a coordinating cation on the surface, which may affect compatibility with the matrix as well as overall performance.[18]

Reagents that react with the sulfate groups of polysaccharides are less explored; however, they may be useful and may have an impact

in biological, medicinal, and material applications. From previous research, it is known that azetidinium salts react preferentially with carboxylates,[19–22] amines,[23,24] phenols,[25] and phosphorus nucleophiles.[26] Azetidinium salts are positively charged, which to some extent governs their adsorption to carboxylic acids via electrostatic interaction. Combined with their inherent four-atom ring strain, this charge makes azetidinium salts reactive under mild conditions. None of the functional groups mentioned above are particularly polar; however, they have large orbitals available for nucleophilic interaction with an electrophile. The sulfate ester has a similar orbital arrangement, especially when compared with carboxylic acids; therefore, it may be suitable for ring-opening reactions with azetidinium salts. Azetidinium conjugation results in a Y-shaped carbon-linked grafting, and is thus a complementary hydrophobization methodology compared with traditional ester and etherification reactions. Azetidinium conjugation may generate new possibilities for the tuning of material properties, since azetidinium ions can be designed in many varieties.

To our knowledge, there are no literature reports on the use of sulfate esters as nucleophiles for the ring opening of azetidinium salts. A reagent that is selective for sulfonate groups will make it possible to enhance suitable properties for use in composites. We have, therefore, investigated the use of azetidinium ions as reagents for sulfated CNCs. Azetidinium salts are easily prepared from epichlorohydrin and dialkyl amines, or by first reacting a monoalkylamine with epichlorohydrin to form an azetidine ring, and subsequently quarternizing the ring with an alkyl group. In this study, two azetidinium salts with 2 or 6 carbon dialkyl substituents were reacted with CNCs with different sulfate content. The substituted CNCs were then used in biocomposite manufacturing with a low-density polyethylene (LDPE) matrix.

EXPERIMENTAL

Materials

The CNCs were prepared from microcrystalline cellulose (MCC) PH-101 (Fluka, Morris Plains, NJ) from a 64% (wt/wt) sulfuric acid solution. Dialysis tubing (Spectra/Por 2 Dialysis Membrane, MWCO 12–14 kDa) was purchased from Spectrum Labs (Los Angeles, CA). All commercial reagents used for the synthesis of *N*,*N*-dialkylazetidinium salts or for modification reactions with CNCs were purchased from Sigma-Aldrich (St. Louis, MO) and were used as received. The *p*-toluenesulfonic acid monohydrate was purchased from Fluka. A linear LDPE (melt index 1.0 g/10 min) from Sigma-Aldrich was used as the matrix for the composites.

Characterization

An atomic force microscopy (AFM) was used to image CNC surface morphology. Measurements were done using a Digital Instruments Nanoscope IIIa equipped with a type G scanner (Digital Instruments Inc., Santa Barbara, CA). The measurements were done in tapping mode and in air using a Micro Masch silicon cantilever NSC 15. Samples for analysis were casted on mica plates from 9 ppm (wt/wt) solutions.

The azetidinium-containing salts along with a model compound were analyzed by nuclear magnetic resonance (NMR). The NMR spectra of the azetidinium salts and the model compound were recorded at 25 °C on a Varian MR-400 (Varian, Palo Alto, CA) operating at −399.95 MHz for proton detection and −100.58 MHz for carbon detection. Dimethyl sulfoxide (DMSO)-d_6 was used as the solvent. Solid-state magic angle spinning (MAS) NMR analyses of the azetidinium-substituted CNCs were performed on a 14.1 T Agilent Inova (Agilent, Palo Alto, CA) with a ^{13}C- and ^{1}H Larmor frequency of −150.9 and −600.1 MHz, equipped with a 3.2 mm double-resonance MAS probe. ^{13}C cross polarization (CP) and ^{13}C insensitive nuclei enhanced polarization transfer (INEPT) were recorded at a MAS rate of 9 kHz using a ^{13}C spectral width of 30.48 kHz, a repetition delay of 3.3 s, 8192 signal accumulations, and the decoupling scheme proton small-phase incremental alternation. The CP time was set to 1 ms, and the delays for INEPT were set to 3.6 and 2.2 ms. The chemical shift was referenced to adamantane.

Fourier-transform infrared (FTIR) spectroscopy was recorded on a Perkin Elmer Frontier FTIR Spectrometer (Waltham, MA) equipped with an attenuated total reflection device. FTIR spectroscopy was analyzed between 4000 and 400 cm^{-1}, and 32 scans were collected.

Raman measurements were performed using a Bruker MultiRAM Fourier-Transform Raman (FT-Raman) spectrometer (Bruker, Billerica, MA) equipped with a Nd:YAG laser (1064 nm) and a liquid-nitrogen-cooled Ge-diode detector. The resolution was 2 cm^{-1} (full width at half maximum), and the Blackman–Harris three-term window function was used for apodization. Experiments were performed at room temperature with an exposure time of 2 h (1000 scans) and a laser power of 400 mW.

Sulfur (%S) and nitrogen (%N) content was measured using elemental analysis provided by the Mikroanalytisches Laboratorium, Kolbe, Germany.

Zeta potential was measured for the different CNC samples before modification with azetidinium ions, to confirm differences in sulfate content. The measurements were done on a Zetasizer Nano ZS (Malvern Instruments, Malvern, UK). This technique is based on laser Doppler velocimetry. The Smoluchowski approximation was used to convert the electrophoretic mobility to zeta potential. The light source was a 50 mW diode-pumped solid-state laser with 532 nm wavelength. All measurements were carried out at 25 °C using DTS1070 disposable folded capillary cells. The samples were stabilized for 120 s inside the device, and five measurements per sample were recorded, with a minimum of 10 runs per measurement.

The thermal stability of the CNC samples was analyzed using thermogravimetric analysis (TGA) with a TGA/differential scanning calorimetry (DSC) 3+ Star System (Mettler Toledo, Columbus, OH). A sample of ∼5 mg was heated from 25 to 500 °C under a N_2 atmosphere and with a heating rate of 5 °C min^{-1}. The extrapolated onset temperature (T_O) was measured from two replicates using the STARe Excellence Software.

An Instron 5565A (Instron, Norwood, MA) was used to measure the tensile properties of the nanocomposites. Hot-pressed nanocomposite films were punched into dog-bone shapes and conditioned at 23 °C and 50% relative humidity before attached to the tensile testing device. The gauge dimension was ∼30 mm × 4.1 mm × 0.4 mm, the cross-head speed was 6 mm min^{-1}

and a 5 kN load cell was used. Five replicates were done for each sample. The tensile testing was done in atmosphere pressure and at ambient temperature. The samples were evaluated with the Bluehill 2 software.

Preparation of *N,N*-Dialkylazetidinium Salts

The synthesis of the *N,N*-dialkylazetidinium salts followed the procedures described in the literature, with some modifications.[27] In general, 0.1 mol of epichlorohydrin was added dropwise to a solution of 0.1 mol secondary amine and solvent. The temperature was kept below 5 °C during the addition of epichlorohydrin. The reaction mixture was stirred for 2–4 days at room temperature. The solution was washed with diethyl ether; next, the solvent was removed by evaporation under reduced pressure. For the synthesis of 1,1′-diethyl-3-hydroxyazetidinium chloride (named AzOH-DEA in this study), diethylamine was used as the secondary amine, with water as the solvent. For the synthesis of 1,1′-dihexyl-3-hydroxyazetidinium chloride (named AzOH-DHA in this study), dihexylamine was used as the secondary amine, with hexane as the solvent.

NMR Analysis of *N,N*-Dialkylazetidinium Salts

The NMR analyses of the *N,N*-dialkylazetidinium salts were as follows:

NMR Analysis of AzOH-DEA Salt.

- ^{1}H-NMR (400 MHz, DMSO-d_6). δ = 6.57, d, J = 4 Hz (O**H**), 4.61, m, J = 4 Hz, 8 Hz (C**H**, ring), 4.40, dd, J = 12 Hz, 8 Hz (C**H**$_2$, ring), 4.09, dd, J = 12 Hz, 4 Hz (C**H**$_2$, ring), 3.46, q, J = 8 Hz, 3.32, q, J = 8 Hz (C**H**$_2$), 1.11, t, J = 8 Hz (C**H**$_3$).
- ^{13}C-NMR (101 MHz, DMSO-d_6). δ = 69.9 (**C**H$_2$, ring), 57.5 (**C**H, ring), 55.45, 53.5 (**C**H$_2$), 7.8, 7.4 (**C**H$_3$) ppm.

NMR Analysis of AzOH-DHA Salt.

- ^{1}H-NMR (400 MHz, DMSO-d_6). δ = 6.76 d, J = 8 Hz (O**H**), 4.62, m, J = 4 Hz, 8 Hz (C**H**, ring), 4.44, dd, J = 12 Hz, 8 Hz (C**H**$_2$, ring), 4.17, dd, J = 12 Hz, 4 Hz (C**H**$_2$, ring), 3.44, m, J = 4 Hz (C**H**$_2$), 3.27, m, J = 4 Hz (C**H**$_2$), 1.48, broad m (C**H**$_2$), 1.27, broad m (C**H**$_2$), 1.24, broad m (C**H**$_2$), 0.86, t, J = 8 Hz (C**H**$_3$) ppm.
- ^{13}C-NMR (101 MHz, DMSO-d_6). δ = 70.84 (**C**H$_2$, ring), 60.41, 58.52 (**C**H$_2$), 57.65 (**C**H, ring), 30.66, 30.63, 25.29, 25.25, 21.87, 21.86, 21.55 (**C**H$_2$), 13.76 (**C**H$_3$) ppm.

Preparation of *N,N*-Dialkyl-3-methoxyazetidinium Salts

To prepare the *N,N*-dialkyl-3-methoxyazetidinium salts, potassium-*t*-butoxide (1.2 g, 11 mmol) was added to AzOH-DEA (1.65 g, 10 mmol) or to AzOH-DHA (2.8 g, 10 mmol) in dichloromethane (10 mL). After 2 min, methyl-*p*-toluenesulfonic acid (2.2 g, 12 mmol) was added and the reaction was stirred for 1 h at room temperature. The reaction was quenched with a small quantity of water (5 mL), and the mixture was concentrated under reduced pressure to yield the crude product. The product was triturated with acetonitrile, filtered, and then concentrated once again under reduced pressure.

NMR Analysis of 1,1′-Diethyl-3-methoxyazetidinium Chloride Salt. The NMR data for 1,1′-diethyl-3-methoxyazetidinium chloride (AzOMe-DEA salt) is as follows:

- ^{1}H-NMR (400 MHz, DMSO-d_6). δ = 4.44, m, J = 4 Hz, 12 Hz (C**H**$_2$, ring), 4.30, m, (C**H**, ring), 4.14, dd, J = 4 Hz, 12 Hz (C**H**$_2$, ring), 3.41, q, J = 8 Hz, 3.34, q, J = 8 Hz (C**H**$_2$), 3.25, s, (C**H**$_3$O), 1.16 & 1.12, t, J = 8 Hz (C**H**$_3$).
- ^{13}C-NMR (101 MHz, DMSO-d_6). δ = 67.7 (**C**H$_2$, ring), 66.9 (**C**H$_2$, ring), 56.6, (**C**H$_3$O), 56.3 (**C**H, ring), 55.8, 54.3 (**C**H$_2$), 8.1, 7.8 (**C**H$_3$) ppm.

NMR Analysis of 1,1′-Dihexyl-3-methoxyazetidinium Chloride Salt. The NMR data for 1,1′-dihexyl-3-methoxyazetidinium chloride (AzOMe-DHA salt) is as follows:

- ^{1}H-NMR (400 MHz, DMSO-d_6). δ = 7.46, d, J = 8 Hz (2H), 7.09, d, J = 8 Hz (2H), 4.45, dd, J = 8, 12 Hz (C**H**$_2$, ring), 4.29, m (C**H**, ring), 4.15, dd, J = 8, 12 Hz (C**H**$_2$, ring), 3.80, b (C**H**$_2$), 3.30, m (C**H**$_3$O), 3.10, m (C**H**$_2$), 2.27 s (C**H**$_2$), 1.47, m (C**H**$_2$), 1.26, m (C**H**$_2$), 0.86, t, J = 6 Hz (C**H**$_3$) ppm.
- ^{13}C-NMR (101 MHz, DMSO-d_6). δ = 67.7 (**C**H$_2$, ring), 66.9 (**C**H$_2$, ring), 56.6, (**C**H$_3$O), 56.3 (**C**H, ring), 55.8, 54.3 (**C**H$_2$), 8.1, 7.8 (**C**H$_3$) ppm.

Model Reaction Using *p*-Toluenesulfonic Acid Monohydrate

Since the conjugation of azetidinium salts to sulfate groups is limited to the number of available surface sulfate groups, the maximum amount of substitution corresponds to one substituent per sulfate group. This corresponds to approximately one substituent per 70 anhydroglucose units (AGU), according to the elemental analysis results regarding sulfur content. Due to the difficulty of confirming the substitution on the cellulose polymer, model reactions using *p*-toluenesulfonic acid were used to study the ring opening of azetidinium salts using NMR analysis. *p*-Toluenesulfonic acid monohydrate (1.9 g, 10 mmol) was placed in a round-bottom flask with 10 mmol AzOH-DEA or AzOH-DHA salt, and with 15 g DMSO/toluene solution (9:1 ratio) as the solvent. The reaction was heated at 90 °C for 24 h with constant stirring. After the reaction, the solvent was removed via bulb-to-bulb distillation to yield 3-(dialkylamino)-2-hydroxypropyl-4-methylbenzenesulfonate. The product was verified by NMR analysis.

NMR Analysis of the Model Compound

The structure of the model compound, 3-(dialkylamino)-2-hydroxypropyl-4-methylbenzenesulfonate, was assigned using ^{1}H, ^{13}C, homonuclear correlation spectroscopy, heteronuclear single quantum coherence (HSQC), and heteronuclear multiple bond correlation (HMBC). From the proton and carbon NMR, it was concluded that both the tosylate and the azetidinium fragments are present in the molecule, and that their shifts are not identical to the shifts from the starting materials. HSQC and HMBC were used to assign the correlation between protons in the molecules.

NMR Analysis for the Reaction with AzOH-DEA.

- ^{1}H-NMR (400 MHz, DMSO-d_6). δ = 7.45, d, J = 8 Hz (C**H**, ring, 4), 7.08, d, J = 8 Hz (C**H**, ring, 3), 4.09, broad multiples (C**H**, 7), 3.63, dd, J = 5 Hz, 11 Hz (C**H**$_2$, 6), 3.60, dd, J = 5 Hz, 11 Hz (C**H**$_2$, 6), 3.14, m, J = 8 Hz (C**H**$_2$, 9), 3.09, m, (C**H**$_2$, 8), 2.25, s (C**H**$_3$, 1), 1.16, J = 8 Hz (C**H**$_3$, R) ppm.
- ^{13}C-NMR (101 MHz, DMSO-d_6). δ = 145.6, 137.7 (**C**H, ring, 2, 5), 128.0, 125.4 (—**C**—, ring, 3, 4), 65.0 (**C**H, 7), 54.1

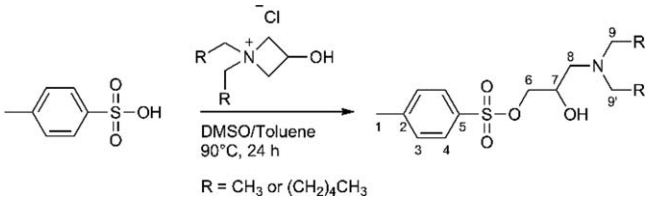

Figure 1. Schematic of the reaction between *p*-toluenesulfonic acid monohydrate and azetidinium salt.

(CH_2, 8), 53.6, 48.0 (CH_2, 9), 48.7 (CH_2, 6), 20.7 (CH_3, 1), 8.6, 8.1 (CH_3, R) ppm. The numbers in parenthesis refer to the molecular structure in Figure 1.

NMR Analysis for the Reaction with AzOH-DHA.

- ^{1}H-NMR (400 MHz, DMSO-d_6). δ = 7.43, d, J = 8 Hz (CH, ring, 4), 7.07, d, J = 8 Hz (CH, ring, 3), 4.10 broad multiplet (CH, 7), 3.63, dd, J = 5 Hz, 12 Hz (CH_2, 6), 3.59, dd, J = 4 Hz, 10 Hz (CH_2, 6), 3.09, m, (CH_2, 8), 3.08, m, (CH_2, 9), 1.61, m, (CH_2, R), 1.25, m, (3× CH_2, R), 0.84, m, (CH_3, R) ppm.
- ^{13}C-NMR (101 MHz, DMSO-d_6). δ = 145.5, 137.6 (CH, ring, 2, 5), 128.0, 125.4 (—C—, ring, 3, 4), 65.0 (CH, 7), 54.6 (CH_2, 8), 53.6, 48.0 (CH_2, 9), 48.7 (CH_2, 6), 31.2 (CH_2, R), 26.5 (CH_2, R), 23.4 (CH_2, R), 22.5 (CH_2, R), 21.84 (CH_3, 1), 14.47 (CH_3, R) ppm.

In the NMR analysis, the ring-opened form of the azetidinium compound was observed at the signals 4.09 (CH, 7) and 3.63, 3.09 (CH_2, 6, 8) ppm, which correspond to the signals at 65.0 (CH, 7) and 48.7, 54.1 (CH_2, 6, 8) ppm in the ^{13}C-NMR.

Preparation of CNCs

CNCs were prepared according to the procedure described by Hasani *et al.*, with adjustments based on the raw material.[14] Aqueous suspensions of CNCs were prepared via the hydrolysis of MCC using 64% (wt/wt) sulfuric acid and continuously stirred at 45 °C for 2 h. The reaction was quenched by threefold dilution with deionized water, immediately followed by centrifugation at 4300 rpm for 15 min to remove the excess acid and water. The supernatant was removed and the precipitate was redispersed in deionized water and re-centrifuged. This was repeated twice, followed by dialysis against deionized water, until the conductivity in the effluent remained below 5 μS. The CNC particles were dispersed by sonication at 40% output until a colloidal suspension was achieved. Rod-like crystals with a length and diameter of ~300 nm × 7 nm were confirmed using an AFM, see Figure 2(c).

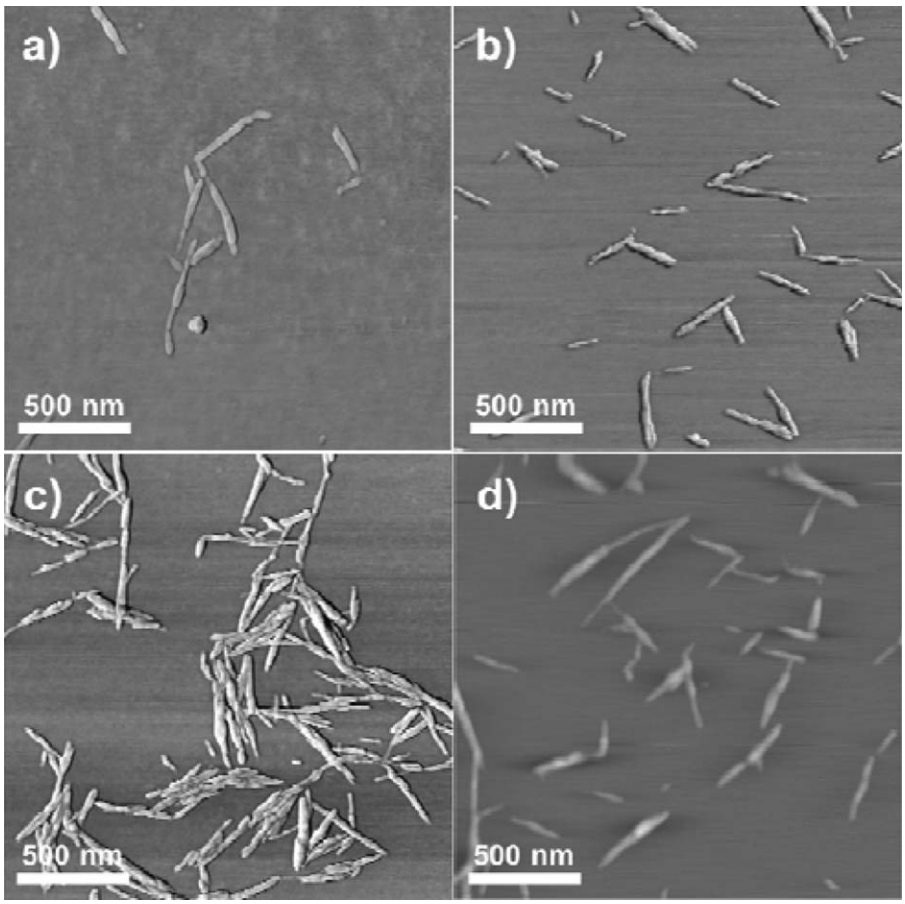

Figure 2. AFM images of the four different CNC samples used in the study: (a) desulfated CNCs (CNC-0), (b) partly desulfated CNCs (CNC-1), (c) sulfated CNCs from the sulfuric acid hydrolysis (CNC-2), and (d) oversulfated CNCs (CNC-3).

Table I. Zeta Potential and Sulfur Content (%S) Measured by Elemental Analysis for the Different CNCs Samples

Sample	Zeta potential of CNC samples before modification	Sulfur content of CNC samples before modification	Sulfur content of AzOH-DEA-modified CNCs	Sulfur content of AzOH-DHA-modified CNCs
CNC-0 (desulf.)	−37.0 mV	0.00%	0.00%	0.02%
CNC-1 (partially desulf.)	−69.5 mV	0.47%	0.00%	0.47%
CNC-2 (original)	−78.3 mV	0.55%	0.00%	0.52%
			0.67%[a]	--
CNC-3 (oversulf.)	−78.6 mV	0.85%	0.15%	0.51%

[a] Data for the CNC-2 sample modified with AzOMe-DEA.
The zeta potential is only measured for the CNC samples before modification with azetidinium salts to confirm differences

Pretreatments of CNCs for Variation in Sulfate Content

Desulfation. Two low-charge CNC samples were prepared according to procedures published earlier, with minor modifications. The procedures are described below.

Acid-Catalyzed Desulfation.[28,29] 200 mL CNC solution (1% wt/wt) was preheated to 80 °C; next, 5 mL of 1 *M* HCl was added and allowed to react at 80 °C with constant stirring for 2.5 h. The reaction was stopped by cooling the reaction flask in an ice bath, followed by centrifugation at 4300 rpm for 15 min and dialyzed against deionized water until the conductivity in the effluent remained below 5 μS. AFM image of the CNC sample is shown in Figure 2(a).

Solvolytic Desulfation.[28,30] 200 mL of CNC solution (1% wt/wt) was neutralized with pyridine (200 mL) and subsequently lyophilized. The freeze-dried CNCs (~2 g) were dispersed in DMSO and sonicated for 2 min at 40% output. Next, 20 mL methanol was added and the mixture was heated at 80 °C for 2 h with constant stirring in a heating bath. The reaction was stopped by cooling the reaction flask in an ice bath. The mixture was centrifuged at 4300 rpm for 15 min, and then the supernatant was removed. The precipitate was re-dispersed and re-centrifuged several times and finally put on dialysis against deionized water. AFM image of the CNC sample is shown in Figure 2(b).

Oversulfation. High-sulfate-charge CNCs were prepared according to the procedures described by Araki *et al.*, with minor modifications.[31] First, 452 g sulfuric acid (64% wt/wt) was mixed with 74 g CNC solution (2.7% wt/wt) and allowed to react for 2 h at 40 °C. The reaction was quenched by dilution in deionized water, immediately followed by centrifugation at 4300 rpm for 15 min. The supernatant was then removed, and the precipitate was re-dispersed and re-centrifuged. This was repeated once, followed by dialysis against deionized water until the conductivity in the effluent remained below 5 μS. AFM image of the CNC sample is shown in Figure 2(d).

Sulfate Content of Pretreated CNC Samples

Different pretreatments were performed on CNCs from a mother batch (CNC-2), and two samples were desulfated to different degrees: one was almost fully desulfated (CNC-0), while another was partially desulfated (CNC-1). A third sample was oversulfated (CNC-3). Table I shows the different sulfur contents (%S) and the zeta potential after the different treatments of CNCs. The sulfur content was measured using elemental analysis, and the value for the original CNC sample (CNC-2) was in the same range as the CNC sulfur content reported by other research groups.[32,33] From Table I, it can be seen that the two samples that were desulfated had lower sulfur content and a higher zeta potential compared with the original CNCs. The oversulfated CNC sample had a higher sulfur content and a slightly lower zeta potential. These results show that the desulfation and oversulfation treatments were successful.

To obtain further proof of the sulfate content, complimentary Raman analysis was performed on a sulfated CNC sample and a desulfated CNC sample. Figure 3 shows the Raman analysis in the wave number range 1000–1200 cm^{-1}, which includes bands corresponding to C—O—C asymmetric stretching, S=O stretching, and SO_2 stretching. There are significant reductions in the band area 1050–1200 cm^{-1}, which represent sulfone groups. Since C—O—C stretching occurs in the same region as sulfate–oxygen stretching, Raman signals are present in that region even though the sulfate content is almost negligible.

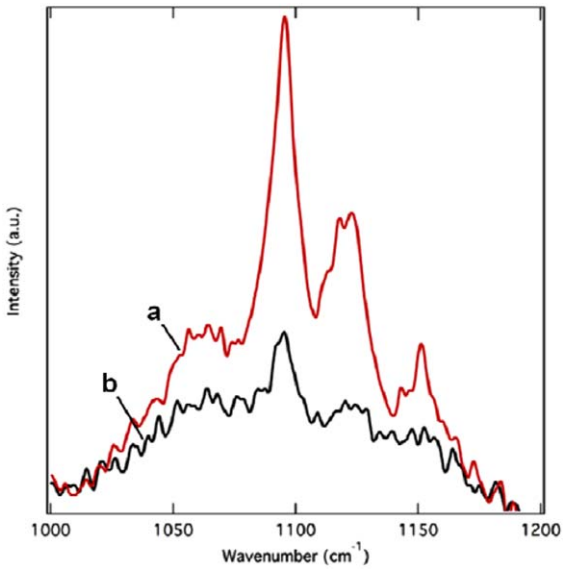

Figure 3. Raman spectroscopy analysis of (a) sulfated CNC (red) and (b) desulfated CNC (black). [Color figure can be viewed at wileyonlinelibrary.com]

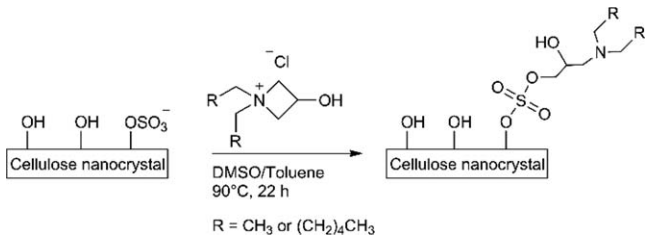

Figure 4. The general reaction scheme between CNC prepared from sulfuric acid and *N,N*-dialkylazetidinium salts.

Modification of CNCs With *N,N*-Dialkylazetidinium Salts

A reaction that was similar to the one used for the model compound, 3-(dialkylamino)-2-hydroxypropyl-4-methylbenzenesulfonate, was used for the reactions of the CNC samples with different sulfate content and for the two *N,N*-dialkylazetidinium salts. Since the literature reports that azetidinium salts can undergo dimerization to 2,5-bis(dialkyl substituted)-1,4-dioxanes in aqueous alkali, a solvent exchange to DMSO was performed on the aqueous CNC solutions through an azeotrope with toluene.[34] An excess of *N,N*-dialkylazetidinium salts (3 mol equiv./AGU) was added to CNCs dispersed in a DMSO/toluene mixture (9:1 ratio), and the reaction was stirred for 22 h at 90 °C. After the reaction, the solution was cooled to room temperature and washed with deionized water and ethanol through repeated centrifugation steps. The modified CNC material was either stored in solutions or dried to thin transparent films. Figure 4 shows a schematic of the azetidinium modification of a CNC.

Production of Nanocomposite Materials

CNC composites were prepared from a hot-melt extrusion by first coating an LDPE powder with CNCs. The LDPE powder was obtained by immersing LDPE pellets into liquid nitrogen and then grinding them to a powder with an average particle diameter of 0.5 mm. The coating was done by heavily shaking a mixture of LDPE powder and aqueous CNC solution, and then by drying the coated LDPE powder at room temperature. The intended concentration after drying was approximately 10 wt % CNCs. A Haake MiniLab twin-screw compounder (Thermo Scientific, Waltham, MA) was used, and was operated at 150 °C and 60 rpm for 5 min. Following extrusion, compression molding into 0.4 mm thick films was performed at 150 °C and under 5 tons of pressure for 5 min. The compression molding was repeated until no air bubbles were observed.

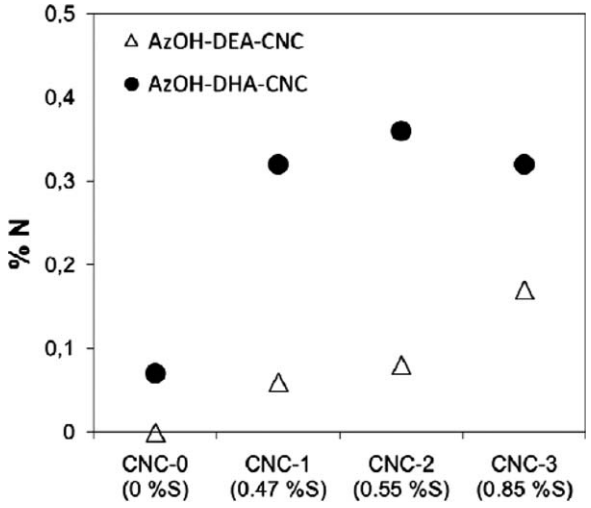

Figure 5. The amount of nitrogen (%N) present in azetidinium-modified CNC samples with different sulfate content.

RESULTS AND DISCUSSION

Azetidinium-Modified CNCs

For the azetidinium-modified CNC samples, one nitrogen atom is introduced per modified site on the nanocrystal. The amount of nitrogen (%N) was measured using elemental analysis, and was then used to evaluate the grafting reaction. Figure 5 shows the relation between nitrogen content and the modified samples of CNCs with varying sulfate content. The sulfur content before and after modification is presented in Table I.

The sulfate concentration was relatively unchanged for the samples that were modified with AzOH-DHA; however, surprisingly, the sulfate content was reduced for the CNC samples that were modified with AzOH-DEA. After an extensive review of the literature, it was found that azetidinium-functionalized phosphorodithioates can undergo intramolecular cyclization.[35] We therefore hypothesized that a similar intramolecular cyclization was causing desulfation of the AzOH-DEA samples, whereas the longer alkyl chains formed an arrangement that hindered the intra-molecular cyclization. Therefore, we performed methylation of AzOH-DEA to produce the AzOMe-DEA salt. To our delight, this reaction resulted in the desired product, as shown by the sulfur content from elemental analysis given in Table I.

Figure 6 shows a suggested mechanism for the intramolecular ring closure of a CNC modified with the different azetidinium salts. The figure has been simplified and does not take into account the possibility that the hydroxyl group on the linker may react with a sulfate group on a glucose unit in close proximity.

Solid-state ^{13}C-NMR experiments based on two different polarization transfer schemes, CP and INEPT, were utilized on the modified CNC samples.[36] Side chains, such as hexyl chains in AzOH-DHA-modified CNCs, may be flexible with a rotational correlation time in nanoseconds, even in the solid state; in contrast, cellulose chains are rigid with a rotational correlation time in milliseconds. However, the ^{13}C-NMR signals belonging to flexible chain segments are absent in a standard CP spectrum, whereas they become visible in an INEPT spectrum. The combination of CP and INEPT reports on the bond mobility of the side chains in the modified CNCs, and hence can reveal additional signals. Figure 7 shows CP (blue in online version) and INEPT (red in online version) spectra for AzOH-DEA [Figure 7(a)], AzOH-DHA [Figure 7(b)], and AzOMe-DEA modification [Figure 7(c)] on the sulfated CNC samples. For the AzOH-DEA sample, only CP signals from the rigid cellulose were detected, as expected, whereas the AzOH-DHA and AzOMe-DEA modifications show both CP and INEPT signals, which arise from the solid cellulose and flexible alkyl chains, respectively.

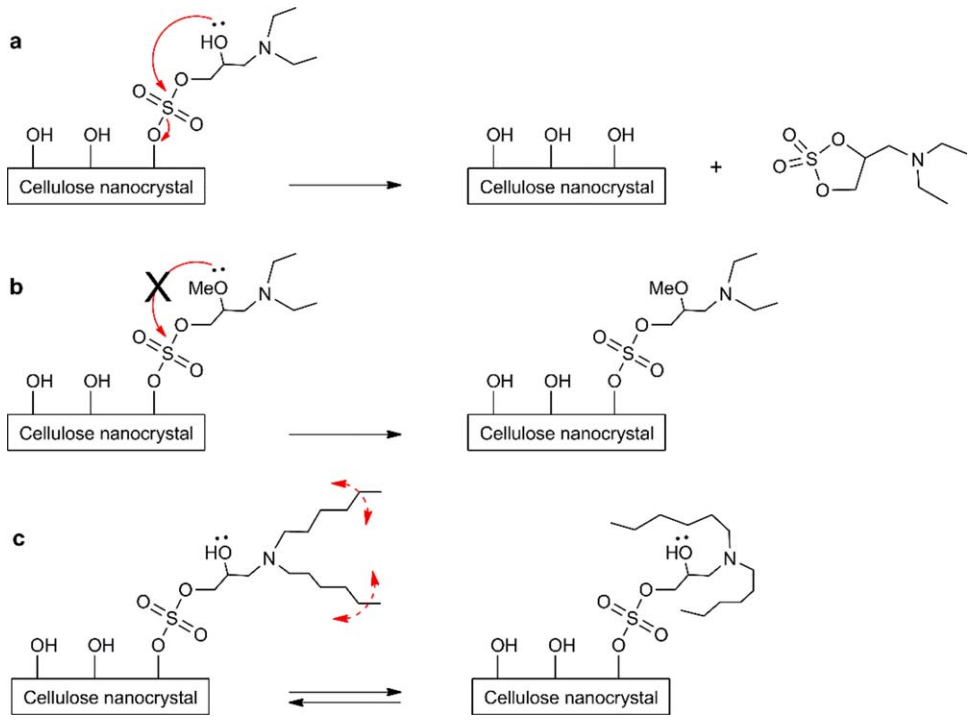

Figure 6. Suggested mechanisms for the modification of CNCs using (a) AzOH-DEA salt, (b) AzOMe-DEA salt, and (c) AzOH-DHA salt. [Color figure can be viewed at wileyonlinelibrary.com]

The CNC samples with different sulfate content and the modified samples were analyzed with FTIR (Figure 8). The CNC samples showed a broad band in the region of 3600–3100 cm^{-1}. This was attributed to O—H stretching that emerged from the vibrations of intra and intermolecular hydrogen-bonded hydroxyl groups. The samples also showed a band area at 2996 cm^{-1}, representing aliphatic saturated C—H stretching in the glucose units.[37] The absorption band at 1052 cm^{-1} shows ring vibrations and stretching vibrations of C—OH side groups, the band at 1161 cm^{-1} represents the glycosidic bonds (C—O—C), and the absorption band at 898 cm^{-1} is typical for β-glycosidic linkage. Other absorption bands detected are 1644 (absorbed water) and 983 (C—O) cm^{-1}.[38] An inconsistency in the differently sulfated CNCs is the presence of the absorption band at 811 cm^{-1}, which is attributed to C—O—S symmetric stretching,[39] whereas the absorption band is present for all CNC samples except the fully desulfated CNC sample (CNC-0). These findings are illustrated in Figure 8 for a fully desulfated sample [Figure 8(a)] and for a sulfated CNC sample [Figure 8(b)]. The FTIR spectrum for the modified CNC samples shows small changes around 2896 cm^{-1}, corresponding to the alkyl chains in the reagents. The C—O—S peak around 811 cm^{-1} is missing in the Az-DEA sample [Figure 8(c)] but not in the AzOMe-DEA-modified [Figure 8(d)] or the Az-DHA-modified [Figure 8(e)] samples. These results correlate with the findings presented in the NMR and elemental analyses.

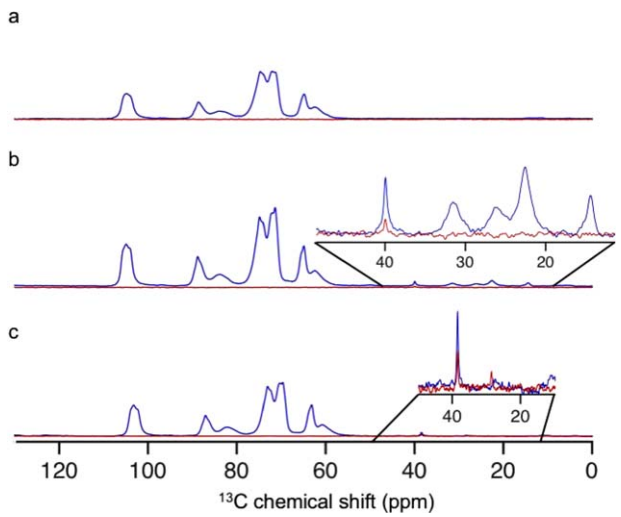

Figure 7. ^{13}C CP (blue in online version) and INEPT (red in online version) NMR spectra of (a) AzOH-DEA-modified CNCs, (b) AzOH-DHA-modified CNCs, and (c) AzOMe-DEA-modified CNCs. [Color figure can be viewed at wileyonlinelibrary.com]

Thermal Stability of Azetidinium-Modified CNCs

The thermal stability of the CNCs and the azetidinium-modified CNCs were evaluated using TGA to measure the degradation onset temperature (T_O). Table II shows the T_O for the four different CNC samples with varying sulfate content and for the different azedtidinium-salt-modifications of the CNC-2 sample. The sulfate groups on the surface of the CNCs lower the thermal stability.[40,41] The sulfate-containing CNC samples (CNC-1, CNC-2, and CNC-3) all have a T_O that is around 155 °C, compared with the fully desulfated sample, which has a T_O of 277 °C (Table II).

Figure 9 shows an example of some TGA graphs where the sulfate content differ or the sulfate groups have been modified

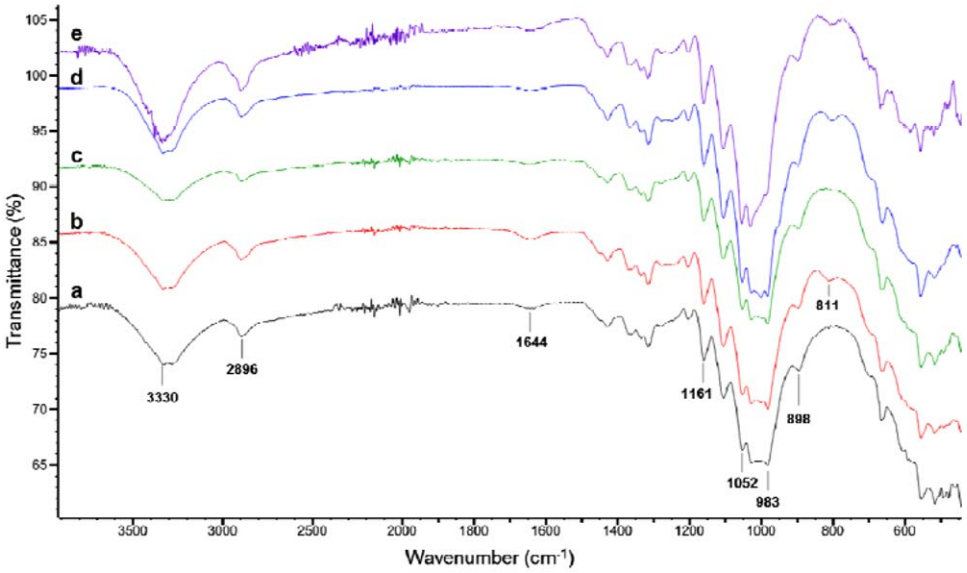

Figure 8. FTIR spectrum for different CNC samples and their modifications. (a) Fully desulfated CNCs (CNC-0), (b) sulfated CNCs (CNC-2), (c) AzOH-DEA-modified CNC-2, (d) AzOMe-DEA-modified CNC-2, and (e) AzOH-DHA-modified CNC-2. [Color figure can be viewed at wileyonlinelibrary.com]

with azetidinium compounds. For the CNC-2 sample in Figure 9, the first temperature degradation (~150 °C) is characterized by the primary pyrolysis of the more accessible and sulfated regions where the sulfuric acid acts as a dehydrating catalyst on the cellulose.[40,42] The consecutive slower process at ~250 °C is suggested to be the charring of the solid residue resulting from the dehydration step.[41] When removing the sulfate groups (CNC-0) the onset thermal degradation temperature shifted to 277 °C, dashed line in Figure 9.

Upon grafting on the sulfate groups in the CNC-2 sample, the T_O shifted from 156 to 246–278 °C for the modified samples. This may be explained by the removal of the acidic hydrogen associated with the sulfate group. The hydrogen is removed through grafting with the azetidinium substituents which thereby hinder the acid-catalyzed dehydration process. Wang *et al.* showed that by replacing the hydrogen ion associated to the sulfate groups with a sodium ion, the acid catalyzed dehydration was inhibited.[41]

Table II. Extrapolated Onset Temperatures Measured with TGA for the Different Sulfate-Containing CNC Samples and for the Azetidinium-Salt-Modifications of the CNC-2 Samples

Sample	Onset temperature (°C)
CNC-0	277 ± 0.2
CNC-1	158 ± 0.2
CNC-2	156 ± 0.0
CNC-3	155 ± 0.2
AzOH-DEA-CNC-2	246 ± 0.3
AzOMe-DEA-CNC-2	278 ± 0.0
AzOH-DHA-CNC-2	250 ± 0.3
AzOMe-DHA-CNC-2	246 ± 0.6

Two replicates were made for each sample

There were no great differences between the methylated and non-methylated azetidinium functionalization for the DHA sample, while a bigger difference was seen between a methylated and non-methylated DEA sample (presented in Table II). The highest T_O was found for the CNC-2 sample that had been functionalized with the AzOMe-DEA reagent. As shown in Figure 6, the methylated groups prevent the intramolecular cyclization while the non-methylated (AzOH-DEA) causes desulfation of the CNCs.

The remaining char is greater for the sulfated CNC samples compared to the desulfated CNCs and the modified samples. This may be explained by the dehydrating action of the sulfate groups which results in a more oxygen deficient char that is less prone to form volatiles.[40] Wang *et al.* showed that the char

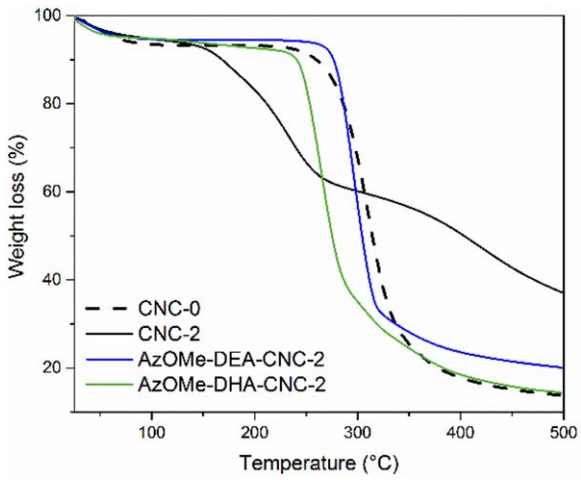

Figure 9. A TGA graph showing the weight loss (%) at different temperatures (°C) for CNC samples without sulfate groups (CNC-0) and with sulfate groups (CNC-2) and, two azetidinium functionalized CNC samples from the CNC-2 sample. [Color figure can be viewed at wileyonlinelibrary.com]

Table III. True Amounts of CNCs in Nanocomposites and Tensile Properties of Different Composites

Sample	Amount CNC (wt %)[a]	Tensile strength (MPa)[b]	Elongation at break (mm/mm)[b]	Young's modulus (MPa)[b]
LDPE	0	25 ± 4	11 ± 2	108 ± 13
Non-modif. CNC + LDPE	3.2	18 ± 1	8 ± 0	216 ± 19
AzOMe-DEA-CNC + LDPE	3.5	14 ± 1	7 ± 0	211 ± 19
AzOMe-DHA-CNC + LDPE	2.9	15 ± 1	7 ± 1	223 ± 11

[a] Measured by TGA.
[b] Measured by tensile test.

decreases when the acidic hydrogen is removed, which may suggest that there are different reaction pathways in the pyrolysis that occur during the TGA measurement.[41]

Nanocomposites

Nanocomposites were prepared through the extrusion of CNC-coated LDPE powder. The true amount of CNCs in the composites could be evaluated from TGA measurements, since CNCs and LDPE decompose at different temperatures. The true amounts of CNCs in the samples are shown in Table III and are around 3 wt %. The nanocomposites showed a visual difference in color (Figure 10), and for the non-modified CNCs, the sample was homogenously black. During extrusion and film pressing, the temperature was kept at 150 °C, which is in the range of the decomposition temperature for CNCs (Table II) due to its sulfate groups. For the two modified samples, the reaction occurred at the sulfate groups, thus protecting the CNC material from degradation at the temperatures used for LDPE composites.

The Y-shaped grafting of CNCs using a similar process to the one described in this study has been reported in the literature.[43] In that study, the researchers used Y-shaped hydrochlorins containing 16–18 carbons, which showed good adhesion to an LDPE matrix after extrusion, and which were suggested to act as a barrier material. In the current work, the mechanical properties were studied as a complement to the barrier properties in the previously mentioned literature.[43] A tensile test was performed on the four different samples shown in Figure 10. The results from the tensile test are reported in Table III showing that the elongation at break and the tensile strength for the nanocomposites is decreased while the Young's modulus increases, compared to a pure LDPE sample. These results correlates with findings in literature saying that addition of a reinforcement can decrease the tensile strength and elongation at break while increasing the Young's modulus.[44] It was also concluded that the modification of the CNCs did not significantly influence the tensile properties of the composite material. By saying that, the azetidinium functionalization keeps the properties of the nanocrystals in a composite matrix but prevents the thermal degradation shown as a discoloring of the material.

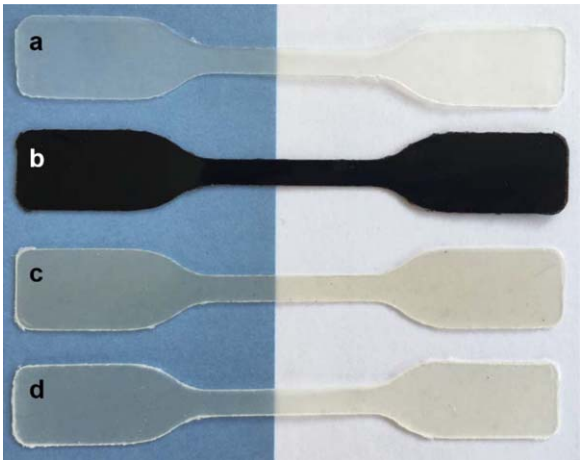

Figure 10. Films made from LDPE composites with (a) pure LDPE, (b) 3.2 wt % non-modified CNC added, (c) 3.5 wt % AzOMe-DEA-CNC added, and (d) 2.9 wt % AzOMe-DHA-CNC added. [Color figure can be viewed at wileyonlinelibrary.com]

CONCLUSIONS

The aim of this study was to show that azetidinium-containing groups in CNCs hydrolyzed from sulfuric acid preferentially react to form sulfonate esters. A model compound using *p*-toluenesulfonic acid monohydrate was characterized with one-dimensional and two-dimensional NMR, showing the ring opening of azetidinium salts. It was used as a reference sample for the polysaccharide reactions. This study shows that sulfate groups can be used as nucleophiles for the ring opening of azetidinium compounds.

Four CNC samples containing different sulfate contents were compared. For CNCs modified with AzOH-DHA, a higher sulfate content resulted in a higher substitution; however, no correlation could be drawn for AzOH-DEA, due to intramolecular cyclization. This intramolecular cyclization could be eliminated by the methylation of the hydroxyl group in the azetidinium salt prior to conjugation to sulfated CNCs.

The reaction between azetidinium ions and CNCs increases the thermal stability of the CNCs by more than 100 °C, according to TGA measurements. The increased thermal stability of the CNC samples increase their suitability for heat-process techniques such as extrusion. A clear difference was seen in the color of the extruded nanocomposites due to the sulfated-induced degradation. The azetidinium-functionalized CNC composites showed equally good mechanical performance, but did not show the severe discoloration.

ACKNOWLEDGMENTS

The authors would like to acknowledge Forskningsrådet Formas and the Knut and Alice Wallenberg foundation for financial support. The research has been carried out in the Swedish research project Smartfoam and in the Wallenberg Wood Science Center (WWSC). The Swedish NMR Centre is acknowledged for spectrometer time and Anders Mårtensson at Applied Polymer Technology (Chalmers University of Technology) is acknowledged for creating the microscopic images.

REFERENCES

1. Chen, G.; Zhang, B.; Zhao, J.; Chen, H. W. *Carbohydr. Polym.* **2013**, *95*, 332.
2. Sanz-Nogues, C.; Horan, J.; Ryan, G.; Kassem, M.; O'Brien, T. *Cytotherapy* **2014**, *16*, S94.
3. Zhu, L. Y.; Yan, X. Q.; Zhang, H. M.; Lin, D. Q.; Yao, S. J.; Jiang, L. *Acta Phys. Chim. Sin.* **2014**, *30*, 365.
4. Wang, Z.; Li, L.; Zheng, B.; Normakhamatov, N.; Guo, S. *Int. J. Biol. Macromol.* **2007**, *41*, 376.
5. Zhang, Y. P.; Sayegh, S. G.; Luo, P.; Huang, S. *J. Fibre Bioeng. Informatics* **2010**, *49*, 3, 32.
6. Dufresne, A. Nanocellulose; From Nature to High Performance Tailored Materials; de Gruyter: Berlin, **2012**.
7. Habibi, Y.; Lucia, L. A.; Rojas, O. J. *Chem. Rev.* **2010**, *110*, 3479.
8. Huang, J.; Chang, P. R.; Lin, N.; Dufresne, A. Polysaccharide-Based Nanocrystals: Chemistry and Applications; Wiley-VCH: Weinheim, **2015**.
9. Hashaikeh, R.; Hu, T.; Berry, R. U.S. Pat. 0,286,387 A1 (**2010**).
10. Doliška, A.; Willför, S.; Strnad, S.; Ribitsch, V.; Kleinschek, K. S.; Eklund, P.; Xu, C. *Holzforschung* **2012**, *66*, 149.
11. Martinichen-Herrero, J. C.; Carbonero, E. R.; Sassaki, G. L.; Gorin, P. A. J.; Iacomini, M. *Int. J. Biol. Macromol.* **2005**, *35*, 97.
12. Pires, L.; Gorin, P. A. J.; Reicher, F.; Sierakowski, M.-R. *Carbohydr. Polym.* **2001**, *46*, 165.
13. Voronova, M. I.; Surov, O. V.; Zakharov, A. G. *Carbohydr. Polym.* **2013**, *98*, 465.
14. Hasani, M.; Cranston, E. D.; Westman, G.; Gray, D. G. *Soft Matter* **2008**, *4*, 2238.
15. Salajková, M.; Berglund, L. A.; Zhou, Q. *J. Mater. Chem.* **2012**, *22*, 19798.
16. Eyley, S.; Thielemans, W. *Nanoscale* **2014**, *6*, 7764.
17. Börjesson, M.; Westman, G. In Cellulose—Fundamental Aspects and Current Trends; Poletto, M., Ed.; InTech: Rijeka, **2015**; p 159.
18. Salas, C.; Nypelö, T.; Rodriguez-Abreu, C.; Carrillo, C.; Rojas, O. J. *Curr. Opin. Colloid Interface Sci.* **2014**, *19*, 383.
19. Espy, H. H. *TAPPI J.* **1995**, *78*, 90.
20. Obokata, T.; Isogai, A. *Colloid Surf. A* **2007**, *302*, 525.
21. Siqueira, E. J.; Salon, M.-C. B.; Belgacem, M. N.; Mauret, E. *J. Appl. Polym. Sci.* **2015**, *132*, DOI: 10.1002/app.42144.
22. Börjesson, M.; Westman, G. *Carbohydr. Res.* **2016**, *428*, 23.
23. Goethals, E. J.; Schacht, E. H.; Bogaert, Y. E.; Ali, S. I.; Tezuka, Y. *Polym. J.* **1980**, *12*, 571.
24. Couty, F.; David, O.; Durrat, F.; Evano, G.; Lakhdar, S.; Marrot, J.; Vargas-Sanchez, M. *Eur. J. Org. Chem.* **2006**, *2006*, 3479.
25. Higgins, R. H.; Faircloth, W. J.; Baughman, R. G.; Eaton, Q. L. *J. Org. Chem.* **1994**, *59*, 2172.
26. Bakalarz-Jeziorna, A.; Heliński, J.; Krawiecka, B. *J. Chem. Soc. Perkin Trans. 1* **2001**, *9*, 1086.
27. Chattopadhyay, S.; Keul, H.; Moeller, M. *Macromol. Chem. Phys.* **2012**, *213*, 500.
28. Jiang, F.; Esker, A. R.; Roman, M. *Langmuir* **2010**, *26*, 17919.
29. Kantor, T. G.; Schubert, M. *J. Am. Chem. Soc.* **1957**, *79*, 152.
30. Usov, A. I.; Adamyants, K. S.; Miroshnikova, L. I.; Shaposhnikova, A. A.; Kochetkov, N. K. *Carbohydr. Res.* **1971**, *18*, 336.
31. Araki, J.; Wada, M.; Kuga, S.; Okano, T. *J. Wood Sci.* **1999**, *45*, 258.
32. Abitbol, T.; Palermo, A.; Moran-Mirabal, J. M.; Cranston, E. D. *Biomacromolecules* **2013**, *14*, 3278.
33. Zhu, J.; Reiner, R. S. U.S. Pat. US8,710,213 B2 (**2014**).
34. Gaertner, V. R. *J. Org. Chem.* **1968**, *33*, 523.
35. Jeziorna, A.; Heliński, J.; Krawiecka, B. *Tetrahedron Lett.* **2003**, *44*, 3239.
36. Gustavsson, S.; Alves, L.; Lindman, B.; Topgaard, D. *RSC Adv.* **2014**, *4*, 31836.
37. Alemdar, A.; Sain, M. *Bioresour. Technol.* **2008**, *99*, 1664.
38. Johar, N.; Ahmad, I.; Dufresne, A. *Ind. Crops Prod.* **2012**, *37*, 93.
39. Abd El Baky, H.; Hanaa El Baz, K.; EL-Latife, S. *J. Aquac. Res. Dev.* **2013**, *5*, 206.
40. Kim, D.-Y.; Nishiyama, Y.; Wada, M.; Kuga, S. *Cellulose* **2001**, *8*, 29.
41. Wang, N.; Ding, E.; Cheng, R. *Polymer* **2007**, *48*, 3486.
42. Roman, M.; Winter, W. T. *Biomacromolecules* **2004**, *5*, 1671.
43. Gårdebjer, S.; Andersson, M.; Engström, J.; Restorp, P.; Persson, M.; Larsson, A. *Polym. Chem.* **2016**, *7*, 1756.
44. Nielsen, L. E. Mechanical Properties of Polymers and Composites; Marcel Dekker, Inc.: New York, USA, **1974**; Vol. *2*.